

# Canonical ensembles and nonzero density quantum chromodynamics

A. Hasenfratz and D. Toussaint

*Department of Physics, University of Arizona, Tucson, AZ 85721, USA*

Received 12 July 1991

(Revised 16 September 1991)

Accepted for publication 17 October 1991

We study QCD with nonzero chemical potential on  $4^4$  lattices by averaging over the canonical partition functions, or sectors with fixed quark number. We derive a condensed matrix of size  $2 \times 3 \times L^3$  whose eigenvalues can be used to find the canonical partition functions. We also experiment with a weight for configuration generation which respects the  $Z(3)$  symmetry which forces the canonical partition function to be zero for quark numbers that are not multiples of three.

## 1. Introduction

Numerical simulations of lattice gauge theory provide a way of studying the behavior of the theory beginning from first principles. The technique is especially useful for studies of the thermodynamics of the strong interactions at high temperatures and zero net quark density. Much less progress has been made at nonzero chemical potential. Credible results at nonzero quark density would provide a testing ground for phenomenological models and possibly be relevant to the structure of neutron stars or relativistic heavy ion collisions.

Finite chemical potential is added to the lattice regularized QCD by multiplying each forward time-like link by  $e^{\mu a}$  and each backward time link by  $e^{-\mu a}$  in the fermionic determinant  $M$  [1]. While  $\det(M(\mu = 0))$  is positive and real,  $\det(M(\mu \neq 0))$  is complex, making standard numerical simulations, normally based on real positive measure, very difficult for the system.

We study QCD at nonzero density by separating the grand canonical partition function  $Z$  into a sum of canonical partition functions  $Z_l$ , where  $l$  is the number of quarks minus the number of antiquarks. Barbour, Davies and Sabeur have shown that the  $Z_l$  can be computed from the eigenvalues of the “propagator matrix”, a sparse matrix of size  $2 \times 3 \times L^3 \times N_t$ , where 3 is the number of colors,  $L$  is the spatial size of the system and  $N_t$  is the euclidean time size of the system [2–4]. In this work we use a smaller, albeit denser, matrix, with size  $2 \times 3 \times L^3$ . Clearly, this

matrix will have a factor of  $N_t$  fewer eigenvalues than the propagator matrix. This condensed matrix is similar to one previously used to compute determinants on  $4^4$  configurations [5].

The expansion of the grand canonical partition function in terms of canonical partition functions was discussed in detail in ref. [3]. The grand canonical partition function of lattice QCD is defined as

$$Z(\mu) = \int dU \det M(\mu) e^{-S_g}, \quad (1)$$

where  $S_g$  is the Wilson gauge action and  $M$  is the fermionic matrix including the chemical potential. For staggered fermions it is

$$\begin{aligned} M(x, y) = & 2am_q \delta_{x,y} + \sum_{\nu=1,2,3} \left( U_\nu(x) \eta_\nu(x) \delta_{x+\hat{\nu},y} - U_\nu^\dagger(y) \eta_\nu(y) \delta_{x-\hat{\nu},y} \right) \\ & + \left( e^{\mu a} U_t(x) \eta_t(x) \delta_{x+\hat{t},y} - e^{-\mu a} U_t^\dagger(y) \eta_t(y) \delta_{x-\hat{t},y} \right). \end{aligned} \quad (2)$$

In the loop expansion  $\det(M)$  is the sum of all possible closed gauge field loops including loops wrapping around the lattice. Each forward wrapping loop in the time direction carries a factor  $e^{-\mu a N_t}$  while the backward wrapping loops carry  $e^{\mu a N_t}$ . All other terms in the loop expansion are independent of the chemical potential. Therefore one can rewrite the grand canonical partition function  $Z$  as a Laplace transform of the canonical partition functions  $Z_l$ , each characterized by the net number of quark loops encircling the lattice in the euclidean time direction and independent of the chemical potential,

$$\begin{aligned} \det(M(\mu)) &= \sum_{l=-l_{\max}}^{l_{\max}} \hat{Z}_l e^{-l\mu a N_t}, \\ Z(\mu) &= \sum_{l=-l_{\max}}^{l_{\max}} Z_l e^{-l\mu a N_t}, \end{aligned} \quad (3)$$

$$Z_l = \int DU \hat{Z}_l e^{-S_g}.$$

Here  $\hat{Z}_l$  is the coefficient of  $e^{-l\mu a N_t}$  in  $\det(M)$  evaluated in a single gauge configuration, while the canonical partition function  $Z_l$  is the weighted average over gauge configurations of  $\hat{Z}_l$ . For  $SU(3)$ ,  $l_{\max} = 3V_s$  where  $V_s = L_x L_y L_z$  is the spatial volume. Henceforth we use units where  $a = 1$ .

From the loop expansion for  $\det(M)$  and the  $\mathbb{Z}(3)$  symmetry of the gauge action (multiply all time direction links on a single time slice by  $e^{\pm i2\pi/3}$ ), it can be seen that  $Z_l = 0$  for  $l \not\equiv 0 \pmod{3}$ . That leaves us with  $V_s$  non-trivial independent

canonical partition functions. Any expectation value in the grand canonical ensemble (eq. (1)) can be expressed through the  $Z_l$ . For example, the average quark density is

$$\langle \rho_q \rangle = \frac{\langle l \rangle}{V} = \frac{\sum_l l Z_l e^{-l\mu N_t}}{\sum_l Z_l e^{-l\mu N_t}}. \quad (4)$$

The fact that  $Z(\mu)$  is a polynomial in powers of  $\exp(\mu N_t)$  with  $2 \times 3 \times L^3$  terms rather than in powers of  $\exp(\mu)$  with  $2 \times 3 \times L^3 N_t$  terms makes it possible to compute the coefficients  $Z_l$  from a matrix of size  $6L^3$ . Because  $Z_l = Z_{-l}^*$  it seems likely to us that the matrix can be further condensed, either to a non-hermitian matrix of size  $3L^3$  or to a hermitian matrix of size  $6L^3$ , which would make finding the eigenvalues even faster.

In eq. (3)  $\det M$  is just the Laplace transform of the  $Z_l$ 's. If we use pure imaginary chemical potential,  $\mu = i\lambda$ ,  $\lambda$  real, eq. (3) will give  $\det M(i\lambda)$  as the Fourier transform of the  $\hat{Z}_l$  and  $Z(i\lambda)$  as the Fourier transform to the  $Z_l$ .

$$Z(i\lambda) = \sum_{-l_{\max}}^{l_{\max}} Z_l e^{ilN_t\lambda}, \quad (5)$$

where

$$Z_l = \frac{N_t}{2\pi} \int_0^{2\pi/N_t} d\lambda e^{-ilN_t\lambda} \int [dU] e^{-S_g} \det M(i\lambda). \quad (6)$$

For imaginary chemical potential,  $\det(M)$  is real and positive. Therefore  $Z_{-l} = Z_l^*$ . The overall normalization of  $Z$  is arbitrary. If we calculate  $\det M$  at  $l_{\max}$  independent values of  $\lambda$ , by Fourier transformation we can get the corresponding  $Z_l$  coefficients. In fact, due to the  $Z(3)$  symmetry,  $Z(i\lambda \pm i2\pi/3N_t) = Z(i\lambda)$ , only  $l_{\max}/3$  values are needed. For smaller volumes (like  $2^4$ ) it is reasonable to calculate the determinant directly at  $l_{\max}/3$  different points. On larger lattices this brute force method becomes very time consuming.

Up to an overall multiplicative constant the canonical partition function coefficients can be calculated using any positive definite measure,

$$Z_l \sim \frac{\int dU \frac{\hat{Z}_l}{W(U)} \frac{W(U) e^{-S_g}}{\int dU W(U) e^{-S_g}}. \quad (7)$$

The simplest choice is to take  $W(U) = \det M(U, \mu = 0)$ , but other measures can be more efficient as we will discuss in sect. 4. For imaginary chemical potential eq. (7) becomes

$$Z_l \sim \int_0^{2\pi/N_t} d\lambda e^{-i\lambda N_t} \frac{\int [dU] \left( \frac{\det M(i\lambda)}{W(U)} \right) W(U) e^{-S_g}}{\int [dU] W(U) e^{-S_g}}. \quad (8)$$

## 2. The reduced matrix and the eigenvalue problem

A simple algebraic transformation reduces the fermionic matrix to a condensed matrix of the size of two time slices whose eigenvalues are simply related to the value of the determinant at any value of the chemical potential.

In the axial gauge,  $U_t(x) = \mathbf{1}$  except at  $t = N_t - 1$ , the fermion matrix can be written in time slices

$$\det(M) = \det \begin{pmatrix} B_0 & \mathbf{1} & 0 & \dots & U_{N_t-1}^\dagger e^{-N_t\mu} \\ -\mathbf{1} & B_1 & \mathbf{1} & \dots & 0 \\ & & \dots & & \\ -U_{N_t-1} e^{N_t\mu} & 0 & \dots & -\mathbf{1} & B_{N_t-1} \end{pmatrix}, \quad (9)$$

where  $B_i$  for  $i = 0, 1, \dots, N_t - 1$  are the spatial derivative and quark mass parts of the matrix at time slice  $i$ , and  $U_{N_t-1}$  denotes the time direction links between slices  $N_t - 1$  and 0. The chemical potential dependence has been transformed to the last time slice. Each entry in the matrix displayed in eq. (9) is itself a matrix of dimension  $L^3$ , each of whose entries is in turn a  $3 \times 3$  complex matrix. Thus the matrix of complex numbers in eq. (9) has dimension  $3 \times L^3 \times N_t$ .

First we multiply the last column by  $U_{N_t-1} e^{N_t\mu}$ . That will change the determinant by a factor of  $\det(U_{N_t-1} e^{N_t\mu}) = e^{V_{N_t} N_t\mu}$ . Next we multiply from the left with the matrix

$$\begin{pmatrix} \mathbf{1} & B_0 & 0 & \dots & \\ 0 & \mathbf{1} & 0 & \dots & \\ & & \mathbf{1} & B_2 & \dots \\ & & & \mathbf{1} & \dots \\ & & \dots & & B_{N_t-2} \\ & & & & \mathbf{1} \end{pmatrix} \quad (10)$$



The matrix  $P$  can also be derived from the propagator matrix [2] by showing that the eigenvalues of the propagator matrix come in  $N_t$ -tuples of the form  $e^{i2\pi j/N_t}C$  for  $j = 0$  to  $N_t - 1$ , and using the identity

$$\prod_{j=0}^{N_t-1} (e^{i2\pi j/N_t}C - x) = C^{N_t} - x^{N_t} \quad (16)$$

to express the characteristic polynomial of the propagator matrix as a polynomial in powers of  $e^{N_t \mu a}$ , which is the characteristic polynomial of the smaller matrix. The smaller matrix is essentially one block of the  $N_t$ th power of the propagator matrix.

### 3. Algorithms

In all our simulations we use four flavors of staggered quarks.

As discussed in sect. 1, the most straightforward procedure is to use the determinant at  $\mu = 0$  in generating configurations. However, this may not be the most efficient procedure. One difficulty with this weight is illustrated by considering how the  $\mathbb{Z}(3)$  symmetry of  $Z(i\lambda)$ , or equivalently the fact that  $Z_l = 0$  for  $l$  not a multiple of 3, is obtained in averaging over configurations. The solid line in fig. 1 represents  $Z(i\lambda)/Z(0)$ , showing the three peaked structure. Most configurations generated with the conventional weight,  $\det(M(0)) e^{-S_g}$ , have  $\det(M(i\lambda))/\det(M(0))$  of the form shown by the lower dashed line, with the maximum at  $\lambda = 0$ . Occasional configurations occur with  $\det(M(i\lambda))/\det(M(0))$  peaked at  $\pm 2\pi/3N_t$ ,

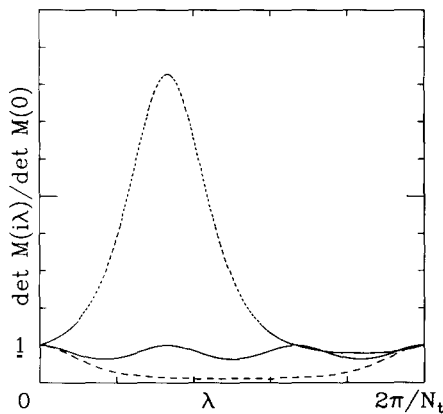


Fig. 1. The solid line shows the expected behavior of  $Z(i\lambda)$  as a function of the imaginary chemical potential  $\lambda$ , showing the  $\mathbb{Z}(3)$  symmetry of this function. The lower dashed line is the contribution to this average from a typical configuration,  $\det(M(i\lambda))/\det(M(0))$ . The upper dashed line is the contribution from one of the rare configurations producing the humps at  $\lambda = 2\pi/3N_t$  and  $2 \cdot 2\pi/3N_t$ .

like the upper dashed line in fig. 1, and these rare configurations provide the other two peaks in the average. Clearly very good statistics are required to obtain an average which really has the  $\mathbb{Z}(3)$  symmetry. In an attempt to get around this problem we have used a probability distribution for configurations which contains this  $\mathbb{Z}(3)$  symmetry. In particular, we use the geometric mean of the determinants at  $\lambda = 0, 2\pi/3N_t$  and  $-2\pi/3N_t$ . Producing configurations with this weight just amounts to simulating with  $4/3$  flavors of quarks at each of these three values of  $\lambda$ . (Remember that for imaginary chemical potential  $\mu = i\lambda$  the determinant remains real and the separation of  $M^\dagger M$  into parts acting on the even sites and on the odd sites is valid.) Thus we generate configurations using the “R” algorithm [6], using three fermionic noise vectors which are inverted using the three different values of  $\lambda$ .

The configurations were generated in single precision, but the link matrices were converted to double precision, and made unitary to double precision, to construct the matrix  $P$ , which was diagonalized in double precision. For calculating eigenvalues we use the QR method, where the matrix is diagonalized by a succession of similarity transformations using  $2 \times 2$  orthogonal matrices [7]. There are a number of empirical checks on the numerical accuracy of the eigenvalues. The  $Z_l$  on each lattice satisfy  $Z_l = Z_{-l}^*$  (This is a good check, because the intermediate steps in the calculation do not manifestly have this symmetry.) The determinant of  $M$  calculated from the  $Z_l$  agrees with the determinant calculated directly (by triangularizing another condensed matrix [5].) Finally, the  $Z_l$  computed on the same lattice on a Cray YMP and a Decstation agree well.

#### 4. Results

We begin our presentation of results with a  $2^4$  lattice, where things are well under control. In fig. 2 we show the  $Z_l$  on a  $2^4$  lattice with  $6/g^2 = 4.0$  and  $m = 0.1$ , where we have measured on 5000 lattices using the  $\mathbb{Z}(3)$  symmetric weight. In this figure the octagons are the value of the  $Z_l$ . Where the  $Z_l$  was negative, we plot its magnitude with a square. Finally, the crosses are statistical error on the  $Z_l$  estimated using the jackknife method. Specifically, we divided the data from each run into about fifty blocks and omitted one block at a time from the calculation, and estimated the error on the result from the variance of the averages over  $N - 1$  blocks, where  $N$  is the number of blocks. It can be seen that the  $Z_l$  for  $l$  not a multiple of three are consistent with zero, while those for  $l$  a multiple of three are an order of magnitude larger than the errors. Fig. 3 shows the density as a function of  $\mu$  constructed from these  $Z_l$ . Again, the errors were estimated using the jackknife method with 50 blocks.

Unfortunately, on  $4^4$  lattices we are still unable to get such convincing results. At a quark mass of 0.05 we have run simulations at  $6/g^2 = 4.8$  and 5.1 using both

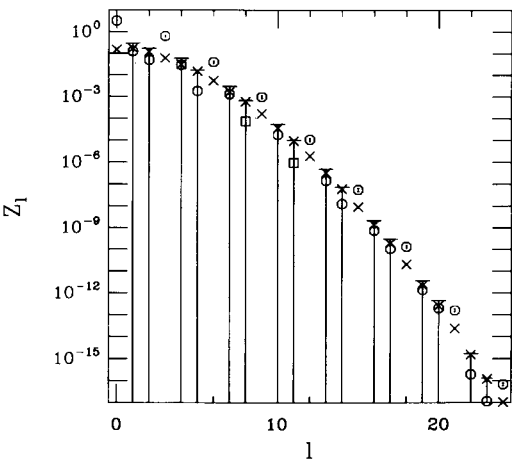


Fig. 2. The  $Z_l$  on a  $2^4$  lattice. The octagons are the  $Z_l$ , the squares are  $-Z_l$ , and the crosses are the statistical errors on the  $Z_l$ .

the conventional action and the  $\mathbb{Z}(3)$  symmetric action. These simulations are in the low- and high-temperatures phases, respectively. We have also performed a simulation at  $6/g^2 = 4.8$  and  $m_q = 0.025$ . Finally, we have done crude hadron spectrum calculations at these values of  $6/g^2$  and  $m_q$  so that we can compare the chemical potential at which the density begins to rise with the pion and nucleon masses.

In the low-temperature runs, we were only able to get statistically significant values for the first nontrivial coefficient  $Z_3$ . However, if we reconstruct the density versus  $\mu$  from the coefficients, estimating errors by the jackknife method, we seem

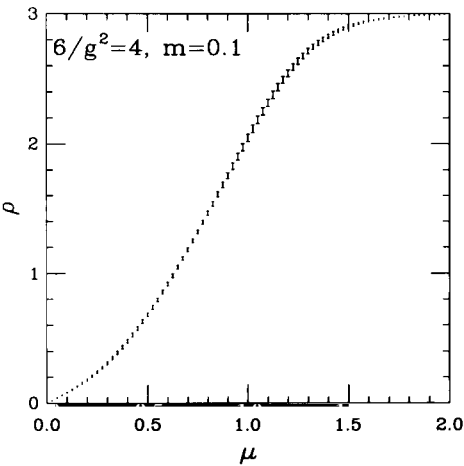


Fig. 3. The quark density per lattice site as a function of chemical potential on the  $2^4$  lattice.



TABLE 1  
The real parts of some  $Z_l$  for a  $4^4$  lattice. Here  $6/g^2 = 4.8$  and  $m_q = 0.05$

Quark number	Conventional weight	$\mathbb{Z}(3)$ symmetric weight
0	1.064(151)	1.364(8)
1	-0.058(79)	-0.000(12)
2	0.012(11)	0.004(3)
3	0.015(6)	0.014(1)
4	$-7(24) \times 10^{-4}$	$-4(4) \times 10^{-4}$
5	$7(6) \times 10^{-4}$	$-4(4) \times 10^{-4}$
6	$6(12) \times 10^{-5}$	$5(4) \times 10^{-5}$
9	$-2(4) \times 10^{-6}$	$1(1) \times 10^{-6}$

to do somewhat better, although the errors on the density are huge over most of the interesting range.

First let us compare the efficiency of the two actions. In table 1 we show the first few  $Z_l$  for a  $4^4$  lattice at  $6/g^2 = 4.8$  and  $m_q = 0.05$ . At this coupling and mass the lattice is “in the confined phase” at  $\mu = 0$ . The run with the conventional weight included 1800 configurations separated by  $1/2$  unit of molecular dynamics time while the run with the  $\mathbb{Z}(3)$  symmetric weight included 5936 configurations. The errors on the  $Z_l$  were estimated using the jackknife method. The errors on the  $Z_l$  from the  $\mathbb{Z}(3)$  symmetric run are much smaller than the errors with the conventional action, even when the effect of the different lengths of the runs, a factor of  $\sqrt{1800/5936} = 0.55$ , is taken into account. With the conventional weight the sum of all the  $Z_l$  normalized as in eq. (8) should be one. This is because at  $i\lambda = 0$  with  $W(U) = \det(M(0))$ ,  $Z(0) = 1$ .  $Z(i\lambda)$  is the Fourier transform of the  $Z_l$ , so its value at 0 is just the sum of the coefficients. With the  $\mathbb{Z}(3)$  symmetric weight the overall normalization is arbitrary.

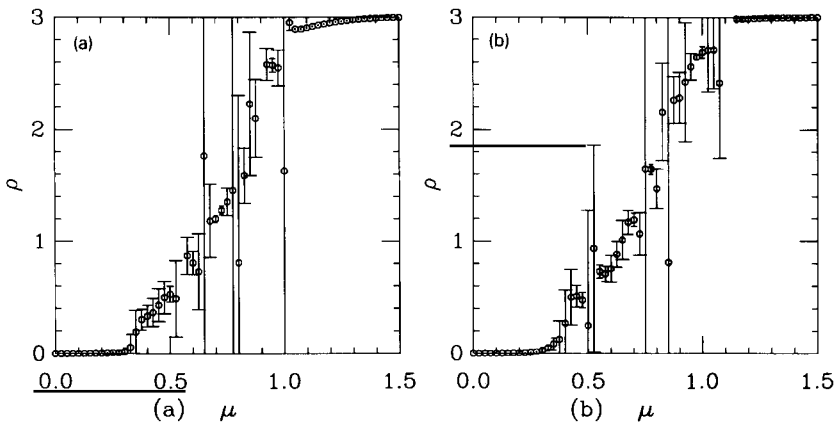


Fig. 4. The quark density per lattice site as a function of chemical potential on a  $4^4$  lattice. Here  $6/g^2 = 4.8$  and  $m = 0.05$ . The density is in units of quarks per lattice site. We show results from (a) the conventional weight and (b) the  $\mathbb{Z}(3)$  symmetric weight.

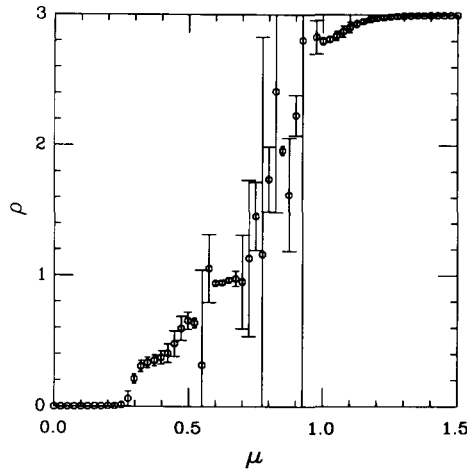


Fig. 5. The quark density per lattice site on a  $4^4$  lattice. Here  $6/g^2 = 4.8$  and  $m = 0.025$ , and the  $\mathbb{Z}(3)$  symmetric weight was used.

In fig. 4 we show the quark density versus chemical potential reconstructed from these coefficients. Here we have used our knowledge of the symmetries to set all the  $Z_l$  for  $l$  not a multiple of three to zero. For both the conventional and the  $\mathbb{Z}(3)$  symmetric weights this makes only a small improvement in the errors on the density. Again, the errors are estimated from the jackknife procedure with about fifty blocks. Strangely, in reconstructing the density the  $\mathbb{Z}(3)$  symmetric weight does not seem to be any better than the conventional weight. Fig. 5 shows the quark density at a quark mass of 0.025. As  $\mu$  increases successively larger  $Z_l$  dominate until for very large  $\mu$  the quark density is saturated at 3, with only the largest  $Z_l$  contributing.

In the high-temperature phase the  $\mathbb{Z}(3)$  symmetry is especially difficult to see in the simulations [3]. Even with the  $\mathbb{Z}(3)$  symmetric weight this remains true, although the situation is improved over the conventional weight. In the case of the conventional weight runs of this length are unlikely to encounter any configurations like the upper dashed line in fig. 1, and in the case of the  $\mathbb{Z}(3)$  symmetric weight the “tunnelings” from one peak to another were too rare to get a good average. Fig. 6 shows the density in the high-temperature phase, showing the very different behavior of the density as a function of  $\mu$ .

To get a rough idea of the mass scale in these simulations we have carried out a conventional calculation of the hadron spectrum on a  $6^3 \times 16$  lattice at  $6/g^2 = 4.8$  and quark masses of 0.05 and 0.025 with four flavors of staggered fermions. We measured hadron propagators on 300 lattices at  $m_q = 0.05$  and 230 lattices with  $m_q = 0.025$ , but the lattices were separated by only one half unit of simulation time. We used the hybrid Monte Carlo algorithm in this simulation. As usual in this strong coupling regime, it is difficult to get a good signal for the  $\rho$  and nucleon

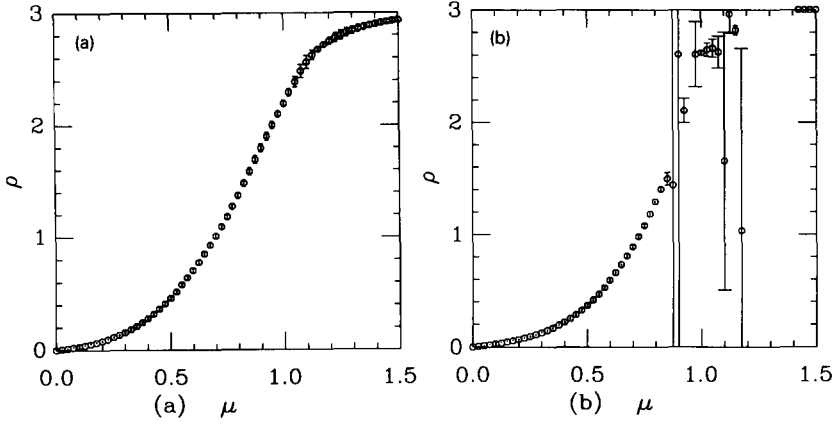


Fig. 6. The quark density per lattice site as a function of chemical potential on a  $4^4$  lattice at high temperature. Here  $6/g^2 = 5.1$  and  $m_q = 0.05$ . We show results from (a) the conventional weight and (b) the  $Z(3)$  symmetric weight.

propagators. At  $m_q = 0.05$  the pion mass is 0.541(2), the  $\rho$ -mass is 1.7(1) and the nucleon mass 2.3(1). At  $m_q = 0.025$  the pion mass is 0.385(2), and we did not obtain reliable results for the  $\rho$  or nucleon. The chemical potential at which a nonzero quark density starts developing,  $\mu \approx 0.3$  for  $m_q = 0.05$  and  $\mu \approx 0.24$  for  $m_q = 0.025$ , is a little larger than one half the pion mass but far below one third of the nucleon mass. (Part of this difference comes from the fact that with four flavors of light quarks the multiplicity of the baryons is fairly large [8].)

We thank Bob Sugar for helpful conversations. Part of this work was carried out while one of us (D.T.) was visiting UCSB and the Institute for Theoretical Physics. This work was supported by the U.S. Department of Energy contract DE-FG02-85ER-40213. Some of the computations were done on the Cray-YMP at the Florida State University Supercomputer Computations Research Institute. The mass spectrum calculation was done on the Ncube 6400 parallel computer at the San Diego Supercomputer Center.

## References

- [1] J. Kogut, H. Matsuoka, M. Stone, H.W. Wyld, S. Shenker, J. Shigemitsu and D.K. Sinclair, Nucl. Phys. B225 (1983) 93;  
P. Hasenfratz and F. Karsch, Phys. Lett. B125 (1983) 308
- [2] I.M. Barbour, C.T.H. Davies and Z.A. Sabeur, Phys. Lett. B215 (1988) 567
- [3] I.M. Barbour and Z.A. Sabeur, Nucl. Phys. B342 (1990) 269
- [4] I.M. Barbour, Nucl. Phys. B (Proc. Suppl.) 17 (1990) 243
- [5] D. Toussaint, Nucl. Phys. B (Proc. Suppl.) 17 (1990) 248
- [6] S. Gottlieb, W. Liu, D. Toussaint, R.L. Renken and R.L. Sugar, Phys. Rev. D35 (1987) 2531
- [7] W.H. Press, B.P. Flannery, S.A. Teukolsky and W.T. Vetterling, Numerical recipes in C (Cambridge Univ. Press, Cambridge, 1988)
- [8] E. Mendel, Nucl. Phys. B (Proc. Suppl.) 20 (1991) 232